Progress in PHOTOVOLTAICS

PROGRESS IN PHOTOVOLTAICS: RESEARCH AND APPLICATIONS
Prog. Photovolt: Res. Appl. 2013; **22:**1237–1244
Published online 22 May 2013 in Wiley Online Library (wileyonlinelibrary.com). DOI: 10.1002/pip.2385

RESEARCH ARTICLE

Broadband light trapping with disordered photonic structures in thin-film silicon solar cells

Angelo Bozzola*, Marco Liscidini and Lucio Claudio Andreani

Dipartimento di Fisica, Università degli Studi di Pavia, via Bassi 6, I-27100 Pavia, Italy

ABSTRACT

We theoretically investigate light trapping with disordered 1D photonic structures in thin-film crystalline silicon solar cells. The disorder is modelled in a finite-size supercell, which allows the use of rigorous coupled-wave analysis to calculate the optical properties of the devices and the short-circuit current density J_{sc}. The role of the Fourier transform of the photonic pattern in the light trapping is investigated, and the optimal correlation between size and position disorder is found. This result is used to optimize the disorder in a more effective way, using a single parameter. We find that a Gaussian disorder always enhances the device performance with respect to the best ordered configuration. To properly quantify this improvement, we calculate the Lambertian limit to the absorption enhancement for 1D photonic structures in crystalline silicon, following the previous work for the 2D case [M.A. Green, Progr. Photovolt: Res. Appl. 2002; **10**(4), pp. 235–241]. We find that disorder optimization can give a relevant contribution to approach this limit. Finally, we propose an optimal disordered 2D configuration and estimate the maximum short-circuit current that can be achieved, potentially leading to efficiencies that are comparable with the values of other thin-film solar cell technologies. Copyright © 2013 John Wiley & Sons, Ltd.

KEYWORDS
light trapping; thin-film silicon solar cells

***Correspondence**
Angelo Bozzola, Dipartimento di Fisica, Università degli Studi di Pavia, via Bassi 6, I-27100 Pavia, Italy.
E-mail: angelo.bozzola@unipv.it

Received 27 July 2012; Revised 28 January 2013; Accepted 13 March 2013

1. INTRODUCTION

In recent years, light trapping with photonic crystal patterns has emerged as a hot research topic to develop high efficiency and low cost thin-film solar cells. Up to now, many efforts have been made for the investigation and optimization of ordered structures, with typical periods comparable with the wavelength of visible light [1–5]. Two physical effects play a major role in these nanopatterned devices: the reduction of reflection losses and the coupling of light to the quasi-guided modes supported by the structures [2,3]. The latter effect is very important, especially for indirect band gap semiconductors such as c-Si, which suffer from poor absorption in the infrared region where the solar irradiance is more intense [6,7]. To quantify the absorption enhancement provided by patterns, a comparison with the Lambertian limit to light trapping is usually performed [8–10]. It turns out that after the optimization of the simple photonic crystal lattices, the overall absorption is still far from the Lambertian limit. In terms of the short-circuit current density J_{sc}, the best results are intermediate between the planar reference configuration and the Lambertian limit [3]. The reason is that for periodic structures, only few diffraction orders can be efficiently exploited for light trapping. Indeed, for a 1D grating of period a, the diffraction cut-off at normal incidence for the mth order in silicon is given by

$$\frac{a}{\lambda} > \frac{m}{n_{Si}} \tag{1}$$

where λ is the wavelength of light and n_{Si} the real part of the refractive index of silicon. Thus, for a = 500 nm (which is the typical optimal period for front patterns [2,3,5]), the maximum number of available modes m is limited to 1 or 2 in the near infrared region. To increase absorption in this region, a broadband optical design with a richer Fourier spectrum is needed. To this end, here we suggest the introduction of a controlled amount of Gaussian disorder in the photonic pattern. The debate about the optimal light-trapping design, in terms of ordered versus random structures, is still open [11–15]. Here, we demonstrate that

an engineered combination of both order and disorder can substantially improve light trapping. In particular, we focus on thin-film c-Si solar cells, which are novel and promising devices where the active material can be obtained via low-cost and epitaxy-free fabrication techniques [16] and then patterned using potentially large-scale nanoimprinting methods [17,18]. In addition, high theoretical limits to the efficiency [6,8–10] are expected for these devices, thanks to broad absorption spectrum and long carriers diffusion lengths. We calculate the optical properties of the photonic structures with rigorous coupled wave analysis (RCWA) [19,20], which is a very suitable tool for the investigation of periodic systems. The effects of disorder are compared with the best results that we obtained for ordered structures in our previous works [2,3]. Only 1D photonic systems are investigated, because it is much harder to reach convergence for the 2D systems. Yet, the physics at the base of light trapping is the same [1,3]; thus, important guidelines can be derived also for the optimization of the 2D systems.

The rest of the paper is organized as follows. In Section 2, we describe the photonic structures under investigation, and in Section 3, we derive an analytical solution for the 1D Lambertian limit, generalizing the treatment of Green [10]. The numerical results are presented in Section 4, where we show the effects of the disorder on the light trapping from a general point of view, analyzing them in the Fourier space framework (Section 4.1). We use these results to optimize the 1D disorder, showing a significant improvement with respect to the ordered configuration (Section 4.2). Finally, we present few comments on the finite-size effects in the modelling of disordered systems using a finite supercell (Section 4.3), and we estimate the maximum achievable short-circuit current in a disordered 2D system (Section 4.4). In Section 5, we sketch our conclusions.

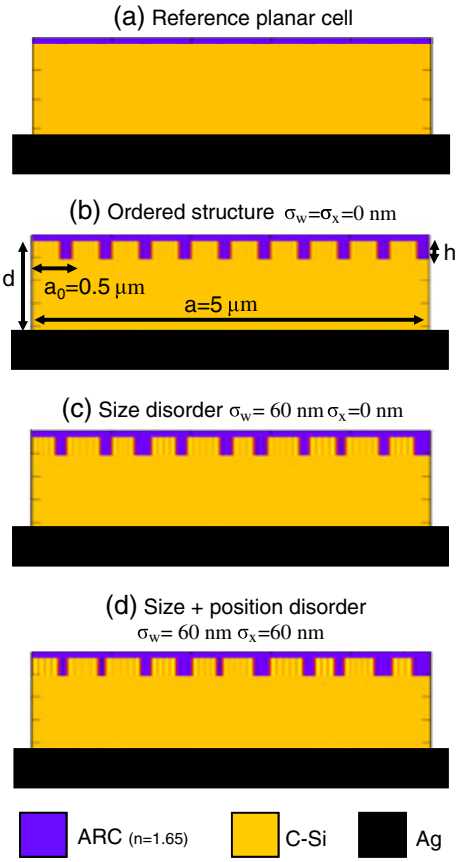

Figure 1. The c-Si solar cells under investigation: (a) the reference planar cell, (b) the optimized ordered configuration, (c) a configuration with size disorder only, and (d) a configuration with both size and position disorder. All the photovoltaic cells have an optimized antireflection layer of thickness 70 nm on the top (n = 1.65 and dispersion less) and a silver back reflector.

2. THE SOLAR CELL STRUCTURES UNDER INVESTIGATION

The structures under investigation are sketched in Figure 1. The reference structure (Figure 1(a)) is a c-Si slab with thickness d = 1 μm, a silver back reflector (the optical functions of the two materials are taken from [7]), and optimized antireflection coating (with thickness 70 nm and refractive index 1.65; see [2]). A silver back reflector is taken in order to be as close as possible to the ideal metallic case (see [21] for a comparative analysis of different back reflectors). We also considered an ordered structure, in which the silicon layer is patterned and the stripes are filled with the antireflection material. Optimization of the periodic pattern gives etching depth h = 200 nm, silicon fraction f_{Si} = 0.7, and period a_0 = 500 nm (Figure 1(b)). To improve light trapping, a controlled amount of Gaussian disorder is introduced in the unit cell, as shown in Figure 1(c,d). In the framework of our Fourier analysis, we consider a supercell of length $a = 10a_0 = 5$ μm containing 10 silicon ridges of width w_i and centred at the position x_i. We notice that another approach based on a supercell with an optimized basis (but with a different silicon thickness) has been recently presented [12]. The use of a supercell allows to model the structure by RCWA, but it introduces a certain approximation in the description of the disorder. In Section 4.3, we will clarify this point. The width of the ith silicon elements is defined as $w_i = w_0 + \Delta w_i$, where the index i runs from 1 to 10, w_0 is the width of the ridge in the optimized periodic 1D lattice, and the quantity Δw_i follows a Gaussian distribution with zero average and standard deviation σ_w:

$$P(\Delta w_i) = \frac{1}{\sqrt{2\pi}\sigma_w} e^{-\Delta w^2/2\sigma_w^2} \tag{2}$$

The central position of the ith silicon element is $x_i = x_{i0} + \Delta x_i$, where x_{i0} is the position of the centre of the ith ridge in the ordered configuration and the quantity Δx_i

DOI: 10.1002/pip

is Gaussian distributed with zero average and standard deviation σ_x:

$$P(\Delta x_i) = \frac{1}{\sqrt{2\pi}\sigma_x} e^{-\Delta x^2/2\sigma_x^2} \quad (3)$$

The etching depth h and the silicon fraction f_{Si} are the same of the ordered configuration. To study the effects of disorder, a statistic analysis over the equivalent structures generated for the same σ_w and σ_x must be performed. In particular, we consider both the average and the best J_{sc} obtained over at least 20 structures with the same σ_x and σ_w. Convergence of the numerical results has been tested for both ordered and disordered structures. In both cases, 101 plane waves with in-plane wave vectors $k_x = k_m = m\frac{2\pi}{a}$ ($a = 5\ \mu m$ and m integer from –50 to +50) are enough for convergence in the investigated spectral range.

3. LAMBERTIAN LIMIT TO LIGHT TRAPPING IN 1D PHOTONIC STRUCTURES

In this section, we derive an analytical expression for the absorption in a c-Si system with an ideal 1D Lambertian scatterer, which is appropriate for a comparison with the investigated structures. We perform the calculation taking into account the actual absorption in the active material: our results generalize the calculations of Green [10] to 1D systems, so we choose to maintain the same notation, when possible.

The 1D Lambertian system is sketched in Figure 2(a): a slab of crystalline silicon with thickness d, (real part of the) refractive index n_{Si}, and absorption coefficient α has a Lambertian scatterer on the front surface and an ideal reflector at the bottom. The photon flux ϕ_{inc} is incident from air and scattered inside the silicon with 1D Lambertian angular distribution function $ADF_{(1D)}$ given by

$$ADF_{(1D)} = \frac{1}{2}\cos\theta \quad (4)$$

where θ is the angle between the z-axis and the scattering direction. The factor 1/2 in Equation (4) derives from normalization of the $ADF_{(1D)}$ for the case of the sole downward scattering. In the 1D case, the light is scattered only along the x direction of Figure 2(a), whereas both the x and y directions are allowed in the 2D case. Many optical quantities are different between the 1D and 2D cases, and we list them in Table I for a comparison. The Lambertian surface is characterized by the hemispherical reflectance R_{ext}, and two hemispherical fluxes ϕ_+ and ϕ_- are defined for the propagation along z inside the silicon. At the Lambertian surface, the relation between ϕ_+ and ϕ_- writes as

$$\phi_- = T_+T_-\phi_+ \quad (5)$$

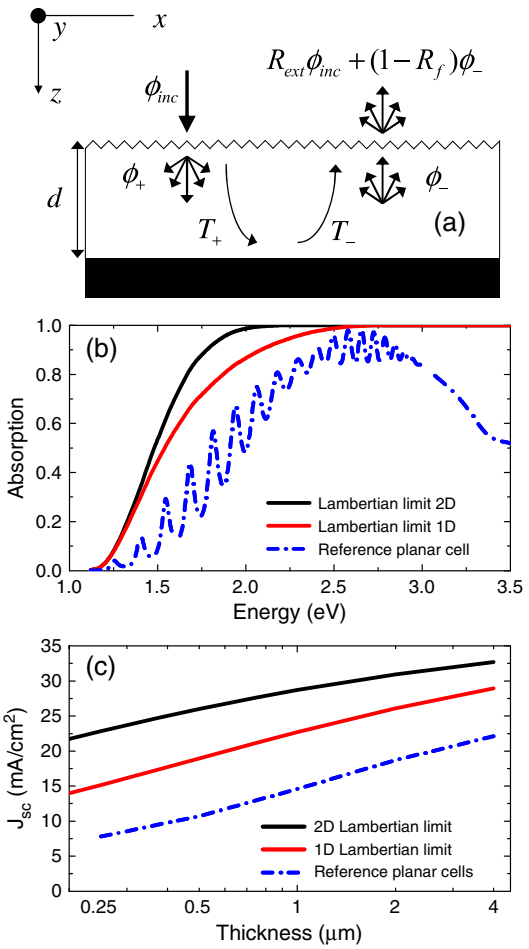

Figure 2. The Lambertian limit to light trapping: (a) solar cell structure used for the calculation of the Lambertian limit and relative notation, (b) comparison between 1D and 2D scattering in terms of the absorption for c-Si with thickness d=1 μm, and (c) short-circuit current density J_{sc}. The same quantities are plotted with dashed-dotted lines for the reference planar cells introduced in Section 2.

Table I. Summary of the differences between the 1D and the 2D Lambertian scatterers.

	1D Case	2D Case
Scattering directions	x only	Both x and y
$ADF(\theta)$	$\frac{1}{2}\cos\theta$	$\frac{1}{\pi}\cos\theta$
$\frac{A}{\alpha d}$ ($\alpha d \to 0$)	πn_{Si}	$4n_{Si}^2$
R_f	$1 - \frac{1}{n_{Si}}$	$1 - \frac{1}{n_{Si}^2}$
J_{sc} for c-Si (d=1 μm)	22.7 mA/cm^2	28.7 mA/cm^2

where $T_+(T_-)$ is the effective transmittance for $\phi_+(\phi_-)$ from the Lambertian surface (bottom) to the bottom (Lambertian surface). Energy conservation at the scattering interface requires

$$\phi_{inc} - \left[R_{ext}\phi_{inc} + (1 - R_f)\phi_-\right] = \phi_+ - \phi_- \quad (6)$$

where $R_f = 1 - 1/n$ is the fraction of light trapped by total internal reflection in the silicon layer, and it is lower than the corresponding 2D quantity (Table I). By combining Equations (5) and (6), the absorption A in the active material can be obtained:

$$A = \frac{(1 - R_{ext})(1 - T_+T_-)}{1 - R_fT_+T_-} \quad (7)$$

The product T_+T_- is calculated from the $ADF_{(1D)}$ and from geometric optics:

$$T_+T_- = \frac{\int_{-\pi/2}^{+\pi/2} e^{-\alpha d/cos\theta} cos\theta \, d\theta}{\int_{-\pi/2}^{+\pi/2} cos\theta \, d\theta} \quad (8)$$

It is worth noticing that when the intrinsic absorption becomes very small ($\alpha d \approx 0$), the absorbance of Equation (7) approaches $\pi n_{Si}\alpha d$, as already pointed out by Fan and co-workers [1] (see also Table I). We numerically evaluated the integral in Equation (8) using the dielectric function of c-Si taken from [7]. The results are shown in Figure 2(b,c) in terms of the absorption and the corresponding J_{sc}. To highlight the role of the light trapping in these idealized systems, we report also the data for the planar reference cells that have no pattern but a single-layer antireflection coating. For simplicity, all the results of this paper are calculated assuming unpolarized light coming from a black body at temperature $T = 5800$ K normalized to an irradiance 100 mW/cm^2 and integrating in the frequency window [1.1,3.5] eV, except otherwise specified (as in Section 4.4). Unit internal quantum efficiency for separation and collection of the photo-generated carriers is always assumed. As expected, the 1D scatterer provides a shorter effective path with respect to the 2D, as a result of monodirectional scattering and less efficient total internal reflection (Table I). Thus, the absorption of a c-Si slab of thickness 1 μm with the 2D scatterer is larger than the corresponding 1D case below 2.5 eV (Figure 2(b)). This difference is amplified for the short-circuit current density, because the low-energy contributions have larger weight as a result of the larger photon flux. The J_{sc} calculated for thicknesses d from 0.25 to 4 μm is shown in Figure 2(c). For all the layer thicknesses considered here, the 1D Lambertian limit is basically intermediate between the 2D case and the planar reference case. We emphasize that we are considering the limit for a given c-Si thickness; that is, we are not using an equivalent material thickness. In the following, we will focus on the thickness $d = 1$ μm, which fits well with the capabilities of the epi-free fabrication techniques for c-Si [16,18] and allows a direct comparison with our previous works on the ordered structures. For this thickness, the 1D Lambertian limit to the J_{sc} is 22.7 mA/cm^2, that is, 6 mA less than the corresponding 2D case.

4. RESULTS

4.1. Light trapping in disordered structures: the role of the Fourier spectrum

We begin the analysis of disorder by calculating the J_{sc} for 20 equivalent structures that are generated for σ_w and σ_x between 0 and 60 nm. This range is limited by the overlap between two consecutive ridges. The average J_{sc} as a function of (σ_w, σ_x) is shown in Figure 3(a). The optimal parameters that maximizes the J_{sc} are $\sigma_w = 50$ nm and $\sigma_x = 25$ nm, and the J_{sc} increases from 19.1 mA/cm^2 (ordered configuration) to 20 mA/cm^2. The spread in the J_{sc} is shown in Figure 3(b)—with the best J_{sc} around 20.3 mA/cm^2. These results can be explained in terms of the richer Fourier spectrum of the disordered structures, which increases the number of accessible diffraction orders, and this is crucial for the absorption enhancement. To obtain a better insight into the physics, we analyzed the features of the contour plot of Figure 3(a) within a Fourier framework, considering also the general properties of the

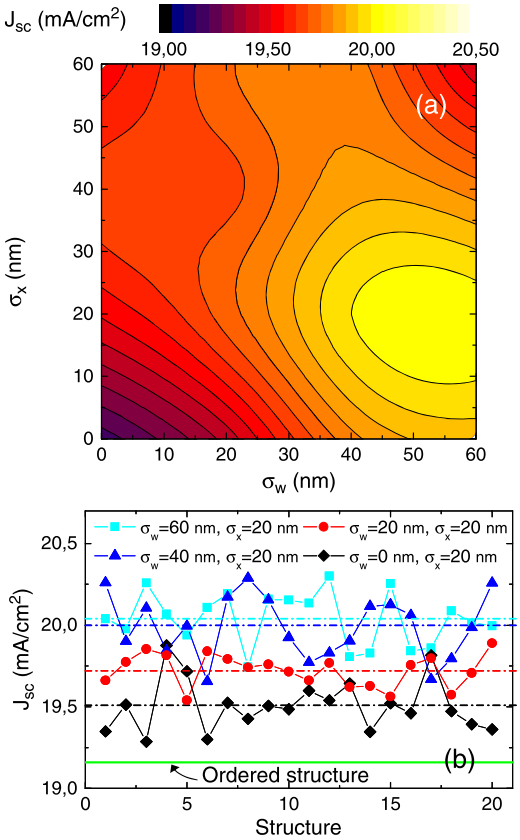

Figure 3. (a) Average short-circuit current density J_{sc} for the disordered structures as a function of σ_w and σ_x. (b) Spread in the J_{sc} for 20 equivalent structures with the same σ_w and σ_x; the average J_{sc} is shown with a dashed line, whereas the value for the ordered configuration is reported with solid line.

DOI: 10.1002/pip

photonic modes in these thin structures. The photonic bands of a planar c-Si slab (n_{Si} = 3.5) with thickness 1 μm in air are calculated using standard waveguide theory [22,23] and reported in Figure 4(a) for the case of transverse electric polarization (electric field along the *y*-axis, parallel to the grating). As we shall see, the differences between this simplified waveguide and the investigated cells are not essential for the following considerations.

The guided modes lie below the air light line and provide a good field confinement in the c-Si. The radiative modes, instead, lie above the air light line and are responsible for diffraction in air. In Figure 4(a), we highlight with a yellow background the spectral range where the absorption of the 1 μm thick c-Si slab is incomplete, that is, where the light trapping is needed. At normal incidence, coupling occurs at the intersections with the photonic bands at $k_x = k_m = m\frac{2\pi}{a}$, as emphasized in Figure 4(a) with black dots for the case of the m = 10 diffraction order. The main parameter affecting the coupling is the strength (amplitude) of the Fourier components of dielectric function in the pattern [11,12,24]

$$|\tilde{\epsilon}(k_m)| = \left|\frac{1}{a}\int_0^a \epsilon(x)e^{-ik_m x}\mathrm{d}x\right| \tag{9}$$

We report the average $|\tilde{\epsilon}(k_m)|$ for different configurations in Figure 4(b,c). For the ordered structure, only the components with m multiples of 10 are active; thus, the coupling to the guided modes is limited. On the contrary, in disordered structures, the strength of the secondary orders increases with σ_w and σ_x, and light trapping is improved. Yet, when the disorder is too large, $\sigma_w = \sigma_x$ = 60 nm, the coupling to the radiative modes close to the zero order is enhanced too, and this limits the J_{sc}. This demonstrate that in the case of Gaussian disorder, the optimal design for light trapping is not a pure random structure with large σ_x and σ_w [11], but it is rather characterized by a finite and relatively small amount of disorder. Similar conclusions for position disorder have been presented in [14]. In addition, size and position disorders have complementary Fourier features. The former enhances the strength of the components that are intermediate between the m = 10 and m = 20 orders. The latter enhances the components close to the main orders and in the radiative zone (Figure 4(c)). This peculiarity favours size disorder over position disorder. The maximum in the contour plot of Figure 4(a) is thus determined by a trade-off between the increased coupling efficiency to the quasi-guided modes, which improves light trapping, and the coupling to the radiative components, which leads to diffraction in air and degrade light trapping when the disorder becomes too large.

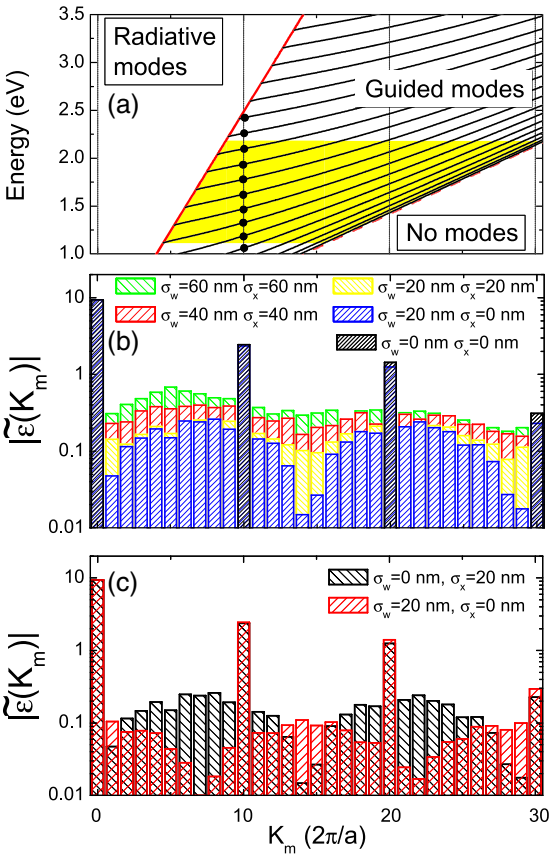

Figure 4. (a) Guided modes of a planar c-Si slab of thickness d = 1 μm in air (no antireflection coating or back reflector are considered). The useful spectral window is highlighted with a light background, whereas the dots define the coupling to the quasi-guided modes mediated by $k_m = 10 \times \frac{2\pi}{a}$ at normal incidence. (b) Strength of the Fourier components of the dielectric function of the 1D patterns of period a=5 μm for different values of σ_w and σ_x, and (c) difference between size and position disorders in terms of their Fourier spectra.

4.2. Correlation in Gaussian disorders

We now turn to the optimization of the disorder for maximizing the J_{sc}. To do that, we first notice that the configurations with high J_{sc} are dislocated along a curve with $\sigma_w\sigma_x$ = constant with an anticorrelation trend, as shown in Figure 3(a). In addition, the optimal correlation is such that $\sigma_w/\sigma_x = 2$. These features suggest that a faster analysis can be performed by defining a single-parameter σ_a for the Gaussian disorder and correlating the size and position disorders. We choose to use the following relations:

$$\sigma_w = f_{Si}\sigma_a \quad \sigma_x = \frac{f_{Si}\sigma_a}{2} \iff \sigma_w\sigma_x = \frac{f_{Si}^2\sigma_a^2}{2} \tag{10}$$

and to investigate 50 equivalent structures with the same σ_a. The best J_{sc} for each σ_a is reported in Figure 5. As for the uncorrelated disorder, the balancing between coupling to the radiative and the quasi-guided modes gives the optimal configuration that maximizes J_{sc}. This optimal disorder parameter is σ_a = 50 nm, with a corresponding J_{sc} = 20.9 mA/cm^2. In terms of short-circuit current, the optimized disorder provides a +43% enhancement with

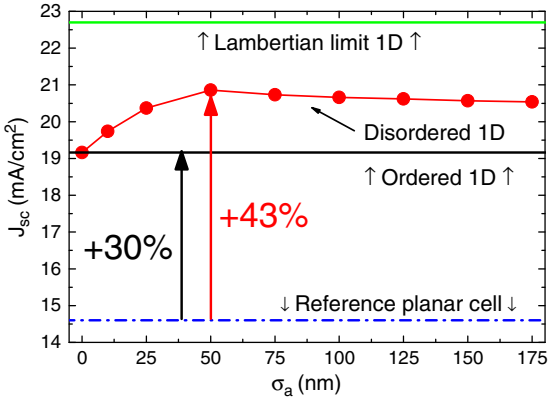

Figure 5. Best short-circuit current density J_{sc} for the structures with correlated disorder varying σ_a, compared with the reference planar cell, the optimized ordered structure, and the corresponding 1D Lambertian limit.

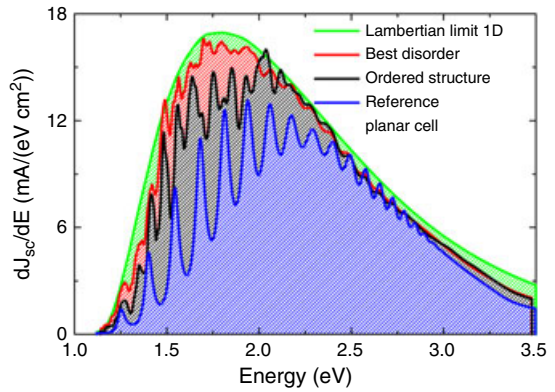

Figure 6. Spectral contributions dJ_{sc}/dE to the short-circuit current density for different structures: for increasing values, the planar reference cell (lowest curve), the optimized ordered structure, the best disordered structure, and the 1D Lambertian limit (highest curve).

respect to the planar reference cell (J_{sc} = 14.6 mA/cm^2). It is also much better than the simple ordered structure and substantially closer to the 1D Lambertian limit.

In Figure 6, we report the spectral contributions dJ_{sc}/dE to the short-circuit current to demonstrate that disorder provides a broadband light trapping. The planar reference case is characterized by complete absorption only above 2.5 eV. The simple 1D pattern provides light trapping and improves the impedance matching, but absorption is still incomplete below 2 eV, and the curve presents deep minima, because only two diffraction orders play a major role at low energy. On the contrary, the richer Fourier spectrum of the optimized disordered structure improves coupling of the incident radiation to the quasi-guided modes over all the investigated spectral range. The resulting curve gives a higher spectral photocurrent, and the deep minima of the ordered configuration almost disappear. The optimized disordered structure is actually very close to the 1D Lambertian limit (green line), and this demonstrates that the introduction of an engineered amount of disorder inside a photonic crystal may be a good solution for high-efficiency light trapping.

4.3. Finite-size effects in disorders optimization

In this section, we spend few words to highlight the effects of a finite supercell in the modelization of the disorder. As already remarked in Section 2, a correct modelization of the disorder would require an infinite supercell period [1]. With RCWA, however, we have to choose a period to define the photonic structure in real space. For a given period and silicon fraction, the degree of freedom of the disordered structures is defined by the number of Fourier components $\epsilon(\tilde{k}_m)$: when the period becomes small, the structure tends to a simple grating. For a larger period, a larger number of Fourier components can be exploited. It is interesting to analyze the effects of light trapping as a function of the period a of the supercell and to understand whether there is a cell size that maximizes the J_{sc}.

In Figure 7, we report J_{sc} for disordered structures with different a. For the case a = 2.5 μm, there are only five c-Si ridges in the supercell. For the a = 10 μm, instead, there are 20 ridges. The average J_{sc} contour plots for the uncorrelated Gaussian disorders (Figure 7(a,b)) have several similarities. First, the optimal configuration is around σ_W=50 nm and σ_X = 20 nm, which is close to the optimal value for the a = 5 μm case. In addition, an anticorrelation trend between size and position disorders is still present. The main difference is the value of the J_{sc}, which slightly increases by increasing the period, when comparing Figures 3(a) and 7(a,b). This trend is observed also for the structures with correlated Gaussian disorder, as shown in Figure 7(c) where the best among the average J_{sc} is shown as a function of the size of the supercell. The value of σ_a that maximizes the J_{sc} is also reported, and it is stable for periods larger than 5 μm. From these results, we conclude that a minimum period a = 5 μm is needed to obtain an appreciable effect of Gaussian disorder. It is worth noticing that, in all cases, convergence with the number of plane waves has been verified.

4.4. Extrapolation of the results to the 2D systems and comparison with the other approaches

In the previous sections, we investigated only 1D photonic patterns, because it is very difficult to achieve convergence in 2D systems using a large supercell. To gain an insight into this problem, in a 1D lattice with period a = 5 μm, up to 101 plane waves are needed for convergence up to 3.5 eV. This number scales linearly with the energy in 1D systems. On the contrary, in 2D systems, the number of involved plane waves scales quadratically with energy: this means that more than 10 000 plane waves would be

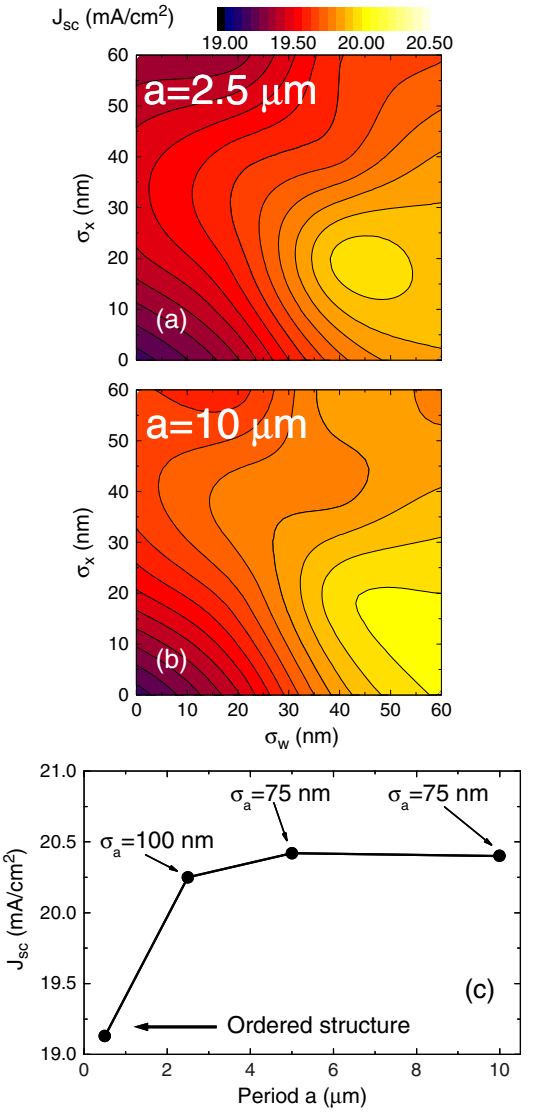

Figure 7. Average short-circuit current density J_{sc} as a function of σ_w and σ_x for disordered structures with different supercell periods (a) a = 2.5 μm and (b) a = 10 μm. (c) The best average J_{sc} for structures with correlated disorder and different periods. The value of σ_a that maximizes the average J_{sc} is also reported.

required for convergence up to the same energy. In addition, the computational time in RCWA scales with the cube of the number of plane waves [19,20], making calculations for 2D disordered systems very difficult. Yet, it is well known that 2D systems can perform much better than 1D for light trapping, as a result of the larger contribution from diffraction [1,3]. In this section, we try to extrapolate the results of Sections 4.1 and 4.2 to 2D photonic structures for estimating the maximum achievable short-circuit current. We did not consider any carrier recombination mechanism that would decrease the J_{sc} in a device. This comparison is useful just to highlight the potentialities of patterned thin-film devices in producing a photocurrent that is comparable with other solar cell technologies.

The first step is to convert the optimal 1D parameters σ_w and σ_x for size and position disorder into the equivalent 2D quantities. To do this, we assume a square lattice of period a_0 = 600 nm and circular rods of radius r_0 = 200 nm as the starting 2D ordered configuration [3]. For the disordered structures, we assume a supercell of period $a = na_0$ containing n^2 rods with positions x_i and y_i and radius r_i. We assume that the rods are filled with the same antireflection coating material used in the rest of the work. The Gaussian position disorder in a 2D system is described by means of two parameters σ_x and σ_y for the x and y directions, respectively.

We can assume that the optimal size disorder scales linearly with the period a_0; thus, the optimal σ_x and σ_y should be equal and around 30 nm for the 2D case. Taking $\sigma_x = \sigma_y$ should be the best choice, because the beneficial effects of disorder would be equal for both the in-plane directions, minimizing the angular and the polarization dependence of the spectral response of the device. The standard deviation σ_w of the 1D case has to be converted into a standard deviation σ_r for the distribution of the radii of the rods for the 2D case. To do this, we assume that the relative size variation induced by the disorder has to be the same in 1D and 2D:

$$\frac{\sigma_w}{w_0} = \frac{\sigma_r}{r_0} \tag{11}$$

Substituting the values for w_0 = 350 nm, σ_w = 50 nm, and r_0 = 200 nm into Equation (11), we can infer the optimal size disorder for the 2D case as $\sigma_r \approx 30$ nm.

We then extrapolate the J_{sc} that would be obtained in the optimized 2D case under AM 1.5 solar spectrum [6]. From the results of Section 4.2, we observe that the best disordered structure (J_{sc} = 20.9 mA/cm^2) is intermediate between the ordered one (J_{sc} = 19.1 mA/cm^2) and the corresponding 1D Lambertian limit (J_{sc} = 22.7 mA/cm^2). Considering that the optimized 2D ordered configuration provides J_{sc} = 22 mA/cm^2 [3] and that the 2D Lambertian limit has J_{sc} = 28.7 mA/cm^2 (Table I), the optimized 2D disordered configuration is expected to have $J_{sc} \approx$ 25 mA/cm^2. We then calculate the optical spectra of the patterned 1D structures up to 4.4 eV and performed the integration with the standard AM 1.5 solar spectrum [6], which is more intense than the black body spectrum in the visible region. This produces a higher short-circuit current density J_{sc} = 24.3 mA/cm^2 for the 1D structure, with a relative +16% increase compared with the results of Section 4.2. This enhancement would produce a short-circuit current density $J_{sc} \approx$ 29 mA/cm^2 for the optimized 2D configuration. We compare these values with those from other established fabrication techniques for crystalline silicon solar cells. Bulk laboratory-size c-Si solar cells typically have larger short-circuit currents ranging between 35 and 40 mA/cm^2, with the record value J_{sc} = 42.7 mA/cm^2 for the PERL solar cell design [25]. Our structures generate a smaller photocurrent, but the quantity of high-quality active material would be reduced by two

orders of magnitude. This demonstrates that the thin-film c-Si solar cells with photonic patterns have the potential to compete with other silicon technologies and that the quantity of active material can be drastically reduced once a proper light-trapping design is used.

5. CONCLUSIONS

We investigated the effects of a Gaussian disorder in c-Si solar cells with 1D photonic patterns for light trapping. We modelled the disorder considering both size and position variations of the pattern, and we investigated the role of the Fourier spectrum for the light trapping. After analyzing the general features of disorder, we made use of the optimal anticorrelation trend between size and position disorder to improve the design. In this way, we optimized the disorder to produce the highest short-circuit current using just one parameter. We found that a controlled and relatively small amount of disorder (σ_w = 50 nm and σ_x = 25 nm or, equivalently, σ_a = 50 nm) has to be introduced in the pattern to maximize light trapping.

Introducing the disorder in the starting ordered configuration always increases the absorption, and the resulting short-circuit current is remarkably close to the 1D Lambertian limit. Extrapolation to the 2D case allows designing optimal configurations and estimating the maximum short-circuit current density that can be achieved. The optimal photonic configuration from the point of view of light trapping is neither perfectly ordered nor totally random, but rather an engineered combination of both order and disorder. The photonic structures considered in this work are easy to realize in a silicon layer with just one lithographic and etching step. The same concept can also be applied to thin-film solar cells made of different materials, for example, amorphous or microcrystalline silicon. The results demonstrate that thin-film crystalline silicon solar cells with photonic structures for light trapping have the potential to compete with other common solar cell technologies.

ACKNOWLEDGEMENT

This work was supported by Fondazione Cariplo under project 2010-0523 'Nanophotonics for thim-film photovoltaics'.

REFERENCES

1. Yu Z, Raman A, Fan S. Fundamental limit of nanophotonic light trapping in solar cells. *Proceedings of the National Academy of Science of the United States of America* 2010; **107**(41): 17491–17496.
2. Zanotto S, Liscidini M, Andreani LC. Light trapping regimes in thin-film silicon solar cells with a photonic pattern. *Optics Express* 2010; **18**(5): 4260–4274.
3. Bozzola A, Liscidini M, Andreani LC. Photonic light-trapping versus Lambertian limit in thin film silicon solar cells with 1D and 2D periodic patterns. *Optics Express* 2012; **20**(S2): A224–A244.
4. Meng X, Drouard E, Gomard G, Peretti R, Fave A, Seassal C. Combined front and back diffraction gratings for broad band light trapping in thin film solar cell. *Optics Express* 2012; **20**(S5): A560–A571.
5. Buencuerpo J, Munioz-Camuniez LE, Dotor ML, Postigo PA. Optical absorption enhancement in a hybrid system photonic crystal – thin substrate for photovoltaic applications. *Optics Express* 2012; **20**(S4): A452–A464.
6. Nelson J. *The Physics of Solar Cells*. Imperial College Press: London, 2003.
7. Palik ED. *Handbook of Optical Constants of Solids*. Academic: Orlando, 1985.
8. Yablonovitch E. Statistical ray optics. *Journal of the Optical Society of America* 1982; **72**(7): 899–907.
9. Yablonovitch E, Cody GD. Intensity enhancement in textured optical sheets for solar cells. *IEEE Transactions on Electron Devices* 1982; **29**(2): 300–305.
10. Green MA. Lambertian light trapping in textured solar cells and light-emitting diodes: analytical solutions. *Progress in Photovoltaics: Research and Applications* 2002; **10**(4): 235–241.
11. Battaglia C, Hsu CM, Söderström K, Escarré J, Haug FJ, Charrière M, Boccard M, Despeisse M, Alexander DTL, Cantoni M, Cui Y, Ballif C. Light trapping in solar cells: can periodic beat random? *ACS Nano* 2012; **6**(3): 2790–2797.
12. Martins ER, Li J, Liu Y, Zhou J, Krauss TF. Engineering gratings for light trapping in photovoltaics: the supercell concept. *Physical Review B* 2012; **86**(4): 041404(R), 1–4.
13. Lin C, Ningfeng H, Povinelli ML. Effect of aperiodicity on the broadband reflection of silicon nanorod structures for photovoltaics. *Optics Express* 2012; **20**(S1): A125–A132.
14. Oskooi A, Favuzzi PA, Tanaka Y, Shigeta H, Kawakami Y, Noda S. Partially disordered photonic-crystal thin film for enhanced and robust photovoltaics. *Applied Physics Letters* 2012; **100**: 181110, 1–4.
15. Vynck K, Burresi M, Riboli F, Wiersma DS. Photon management in two-dimensional disordered media. *Nature Materials* 2012; **11**: 1017–1022.
16. Depauw V, Qiu Y, Van Nieuwenhuysen K, Gordon I, Poortmans J. Epitaxy-free monocrystalline silicon thin film: first steps beyond proof-of-concept solar cells. *Progress in Photovoltaics: Research and Applications* 2002; **19**(7): 844–850.
17. Herman A, Trompoukis C, Depauw V, El Daif O, Deparis O. Influence of the pattern shape of front-side

periodically patterned ultrathin crystalline silicon solar cells. *Journal of Applied Physics* 2012; **112**: 113107, 1–8, (2012).
18. Trompoukis C, El Daif O, Depauw V, Gordon I, Poortmans J. Photonic assisted light trapping in ultrathin crystalline silicon solar cells by nanoimprint lithography. *Applied Physics Letters* 2012; **101**: 103901, 1–4.
19. Whittaker DM, Culshaw IS. Scattering-matrix treatment of patterned multilayer photonic structures. *Physical Review B* 1999; **60**(4): 2610–2618.
20. Liscidini M, Gerace D, Andreani LC, Sipe JE. Scattering-matrix analysis of periodically patterned multilayers with asymmetric unit cells and birefringent media. *Physical Review B* 2008; **77**(3): 035324, 1–11.
21. Kroll M, Fahr S, Helgert C, Rockstuhl C, Lederer F, Pertsch T. Employing dielectric diffractive structures in solar cells – a numerical study. *Physica Status Solidi A* 2008; **205**(12): 2777–2795.
22. Sheng P, Stepleman RS, Sanda PN. Exact eigenfunctions for square-wave gratings: application to diffraction and surface-plasmon calculations. *Physical Review B* 1982; **26**(6): 2907–2916.
23. Catchpole KR. A conceptual model of the diffuse transmittance of lamellar diffraction gratings on solar cells. *Journal of Applied Physics* 2007; **102**(1): 013102, 1–8.
24. Mallick SB, Agrawal M, Peumans P. Optimal light trapping in ultra-thin photonic crystal crystalline silicon solar cells. *Optics Express* 2012; **18**(6): 5691–5706.
25. Green MA, Emery K, Hishikawa Y, Warta W, Dunlop ED. Solar cells efficiency tables (version 39). *Progress in Photovoltaics: Research and Applications* 2012; **20**(1): 12–20.